Familial Alzheimer's disease-linked presenilin mutants and intracellular Ca^{2+} handling: A single-organelle, FRET-based analysis

Elisa Greotti[a,b,1], Paola Capitanio[b,1], Andrea Wong[b,c], Tullio Pozzan[a,b,d], Paola Pizzo[a,b,*], Diana Pendin[a,b]

[a] Neuroscience Institute – Italian National Research Council (CNR), 35131 Padua, Italy
[b] Department of Biomedical Sciences, University of Padua, Via U. Bassi 58/B, 35131 Padua, Italy
[c] Aptuit an Evotec company, Via Fleming 4, 37135 Verona, Italy
[d] Venetian Institute of Molecular Medicine, 35131 Padua, Italy

ARTICLE INFO

ABSTRACT

An imbalance in Ca^{2+} homeostasis represents an early event in the pathogenesis of Alzheimer's disease (AD). Presenilin-1 and -2 (PS1 and PS2) mutations, the major cause of familial AD (FAD), have been extensively associated with alterations in different Ca^{2+} signaling pathways, in particular those handled by storage compartments. However, FAD-PSs effect on organelles Ca^{2+} content is still debated and the mechanism of action of mutant proteins is unclear.

To fulfil the need of a direct investigation of intracellular stores Ca^{2+} dynamics, we here present a detailed and quantitative single-cell analysis of FAD-PSs effects on organelle Ca^{2+} handling using specifically targeted, FRET (Fluorescence/Förster Resonance Energy Transfer)-based Ca^{2+} indicators. In SH-SY5Y human neuroblastoma cells and in patient-derived fibroblasts expressing different FAD-PSs mutations, we directly measured Ca^{2+} concentration within the main intracellular Ca^{2+} stores, *e.g.*, Endoplasmic Reticulum (ER) and Golgi Apparatus (GA) medial- and trans-compartment. We unambiguously demonstrate that the expression of FAD-PS2 mutants, but not FAD-PS1, in either SH-SY5Y cells or FAD patient-derived fibroblasts, is able to alter Ca^{2+} handling of ER and medial-GA, but not trans-GA, reducing, compared to control cells, the Ca^{2+} content within these organelles by partially blocking SERCA (Sarco/Endoplasmic Reticulum Ca^{2+}-ATPase) activity. Moreover, by using a cytosolic Ca^{2+} probe, we show that the expression of both FAD-PS1 and -PS2 reduces the Ca^{2+} influx activated by stores depletion (Store-Operated Ca^{2+} Entry; SOCE), by decreasing the expression levels of one of the key molecules, STIM1 (STromal Interaction Molecule 1), controlling this pathway.

Our data indicate that FAD-linked PSs mutants differentially modulate the Ca^{2+} content of intracellular stores yet leading to a complex dysregulation of Ca^{2+} homeostasis, which represents a common disease phenotype of AD.

1. Introduction

Alzheimer's disease (AD) is the most common neurodegenerative disease characterized by a progressive neuronal loss in specific brain regions, such as hippocampus and amygdala. The main widely accepted hypothesis for AD pathogenesis, the "amyloid cascade", considers the

toxicity exerted by the β-amyloid (Aβ) peptide as the key event leading to neuronal death [1]. However, AD pharmacological therapies focused on contrasting the process of Aβ peptides accumulation have failed to block the progression of the disease in all its characteristic alterations [2,3], strongly supporting the existence of other factors underlying AD pathogenesis. Indeed, AD patients show other early cell alterations, much less investigated, including deregulated Ca^{2+} homeostasis [4].; is a key second messenger in neuronal pathophysiology and alterations in cellular Ca^{2+} is a key second messenger in neuronal pathophysiology and alterations in cellular Ca^{2+} levels are responsible for neuronal dysfunction and cell death in a number of neurodegenerative diseases [5–7]. As far as AD is concerned, it has been shown that mutations in presenilin (PS) genes, responsible for ~90% of familial AD (FAD) cases [8], impact on several aspects of cellular Ca^{2+} homeostasis, independently of their γ-secretase activity [6,9,10]. In particular, several groups reported that PSs are able to modify Endoplasmic Reticulum (ER) Ca^{2+} handling when expressed in cell lines, however no consensus has been reached about their mechanisms of action and final effect [9,10]. Moreover, Ca^{2+} influx from extracellular milieu also appears to be regulated by PSs. In particular, the Ca^{2+} influx activated by intracellular Ca^{2+} store depletion, the so-called Store-Operated Ca^{2+} Entry (SOCE [11]) has been reported to be decreased in different FAD-PS expressing cells [12–18]; Althoughan imbalance in Ca^{2+} homeostasis has been proposed to represent an early event in the pathogenesis of FAD [16,19,20], the mechanisms through which FAD-linked PS mutants affect Ca^{2+} homeostasis are still controversial. In particular, the role of FAD-PSs in Ca^{2+} handling managed by intracellular storage compartments is highly debated. Organelle Ca^{2+} content in cells expressing FAD-linked PSs has been measured mainly indirectly [21,22] and/or in cell populations [13,16,23], and most often in cells overexpressing PSs [24,25]. A direct, single-cell, measurement of Ca^{2+} concentration ($[Ca^{2+}]$)inside the ER has been performed only few times, analysing the effect of PSs knock-out (KO) or FAD-PS1 mutants expression using D1ER, an ER-targeted Ca^{2+} sensor [26,27]. This probe, however, has a relatively high affinity for Ca^{2+} and, accordingly, at the high $[Ca^{2+}]$ typical of the ER, small variations in cation concentration are difficult to evaluate. A lower affinity, ER-targeted Ca^{2+} probe has been developed by our group [28] and already used to evaluate ER Ca^{2+} content in a cell line expressing a FAD-PS2 mutant [28], neurons from FAD-PS2 transgenic mice [29] and neurons, PC12 and SH-SY5Y cells in response to Aβ oligomers treatment [30]. Here we present a detailed and quantitative single-cell analysis of PSs effects on cellular Ca^{2+} homeostasis. In particular, we compared the effects of wild type (wt) or mutated PSs overexpression in the neuroblastoma cell line SH-SY5Y with those of FAD-linked PSs mutants, expressed at physiological levels, in patient-derived fibroblasts. We directly measured $[Ca^{2+}]$ within ER and Golgi apparatus (GA) sub-compartments, using selectively localized, Fluorescence/Förster Resonance Energy Transfer (FRET)-based probes (ER: D4ER; [28],medial-GA: medialGo-D1cpv [31]; and trans-GA: Go-D1cpv [32];), or in the cytosol (by the D3cpv probe [33];). We unambiguously demonstrate that the expression of FAD-PS2 mutants, but not FAD-PS1, in either SH-SY5Y cells or FAD patient-derived fibroblasts, is able to alter Ca^{2+} handling of ER and medial-GA, but not trans-GA, reducing the $[Ca^{2+}]$ within these organelles, compared to those of control cells. The molecular target of this FAD-PS2 effect is the Sarco/Endoplasmic Reticulum Ca^{2+}-ATPase (SERCA) pump. On the other hand, the expression of both FAD-PS1 and -PS2 affects Store-Operated Ca2+Entry (SOCE), reducing it by decreasing STromal Interaction Molecule 1 (STIM1) expression levels. The importance of these findings for AD pathogenesis are discussed.

2. Materials and methods

2.1. Cell culture and transfection

SH-SY5Y cells were grown in DMEM (Dulbecco's Modified Eagle Medium) containing 10% FCS (Fetal Calf Serum), supplemented with L-glutamine (2 mM), penicillin (100 U/ml), and streptomycin (100 μg/ml), in a humidified atmosphere containing 5% CO_2.

Human fibroblasts were obtained from Coriell Institute for medical research: FAD-PS2-N141I (AG09908, female 81 years old, German); control for PS2 (AG08525, female 82 years old, German); FAD-PS1-A246E (AG06840, male, 56 years old, Canadian); control for PS1 (AG08539, male 54 years old, German). Fibroblasts were grown in DMEM containing 20% FCS, supplemented with L-glutamine (2 mM), penicillin (100 U/ml) and streptomycin (100 μg/ml), in a humidified atmosphere containing 5% CO_2.

Cells were seeded onto glass coverslips (18 mm diameter) in 12-well plates for imaging experiments, or in 6-well plates for Western blot analysis. Transfection was performed at 60–70% confluence with 1 μg of DNA (0.25 μg of Cameleon codifying cDNAs and 0.75 μg of pcDNA3 or PSs codifying cDNAs) using Lipofectamine 2000 Transfection Reagent (Life Technologies) for SH-SY5Y or by electroporation using the Neon Transfection System (MPK500, Invitrogen) for fibroblasts. FRET measurements and Western blots were usually performed 24 h after transfection.

2.2. Ca^{2+} measurements

Live cells expressing the fluorescent probes were analysed using a DM6000 inverted microscope (Leica Microsystems, Germany) with a 40X oil objective (HCX Plan Apo, NA 1.25). Excitation light produced by a 405 nm LED (Led Engin #LZ1-00UA00 LED) was filtered at the appropriate wavelength (410 nm) through a band pass filter (420/20 nm), and the emitted light was collected through a beam splitter (OES, Padua, Italy), emission filters HQ 480/40 M (for Enhanced Cyan Fluorescent Protein, ECFP) and HQ 535/30 M (for citrine/cpV-YFP); dichroic mirror 515 DCXR. The beam splitter permits the collection of the two emitted wavelengths at the same time, thus preventing artefacts due to movement of the organelles. All filters were from Chroma Technologies (Bellow Falls, VT, USA). Images were acquired using an IM 1.4C cool camera (Jenoptik Optical Systems) attached to a 12-bit frame grabber. Synchronization of the excitation source and the cool camera was performed through a control unit run by a custom-made software package, Roboscope (developed by Catalin Dacian Ciubotaru at VIMM, Padua, Italy). Exposure time varied from 100 ms to 200 ms, depending on the intensity of the fluorescent signal of the cells analysed. Frequency of image capture depends on the speed of fluorescence changes we were detecting: usually images are acquired every second.

During the experiment, cells plated on coverslips were mounted into an open-topped chamber thermostated at 37 °C and maintained in an extracellular medium, composed by modified Krebs-Ringer Buffer (mKRB) containing in mM: 140 NaCl, 2.8 KCl, 2 $MgCl_2$, 1 $CaCl_2$, 20 HEPES, 11 glucose, pH 7.4, at 37 °C. All media were perfused through a temperature controller (Warner Instruments, TC-324B) set to have a constant temperature of 37 °C within the chamber.

For store Ca^{2+} content evaluation, cells were firstly perfused with mKRB containing 1 mM $CaCl_2$; after perfusion with 300 μM EGTA, cells were stimulated by perfusion of bradykinin (BK, 100 nM) and/or cyclopiazonic acid (CPA, 20 μM); thereafter, the Ca^{2+} ionophore ionomycin (1 μM) was applied (not with the D4ER probe) to completely discharge the stores; finally digitonin (40 μM, to obtain plasma membrane permeabilization) in Ca^{2+}-free intracellular-like medium (130 mM KCl, 10 mM NaCl, 1 mM $MgCl_2$, 2 mM succinic acid and 20 mM HEPES, 7 pH, at 37 °C) and then a saturating $CaCl_2$ concentration (3 mM) were applied. To prevent gross morphological changes of the ER upon cell permeabilization, dextran (5%) has been added to the intracellular-like medium.

For Ca^{2+} pumping experiments, a Ca^{2+}-buffered solution was prepared by adding to the intracellular medium: 1 mM H-EDTA, 1 mM $MgCl_2$, 2 mM EGTA and 350 μM $CaCl_2$. The free $[Ca^{2+}]$ (100 nM) was estimated by Maxchelator 2.5 and checked by fluorimetric

measurements with fura-2 free-acid. 200 μM ATP-Na salt was added to this Ca^{2+}-buffered solution at the beginning of the experiment.

For SOCE activation, cells were pre-treated with the irreversible SERCA inhibitor thapsigargin (100 nM) for 7 min in a Ca^{2+}-free, EGTA (600 μM)-containing medium; cells were then perfused with the same medium without the inhibitor and challenged with $CaCl_2$ (1.5 or 3 mM). Where indicated, extracellular-like medium was substituted with K^+-based medium (in mM: 5 NaCl, 130 KCl, 2 $MgCl_2$, 3 $CaCl_2$, 10 HEPES, 11 glucose, pH 7.4 at 37 °C).

2.3. Ca^{2+} imaging experiments analysis

Off-line analysis of FRET experiments was performed using ImageJ software. Circularly permuted Venus (cpV) or citrine and ECFP images were subtracted of background signals and proper regions of interest (ROIs) were selected on each imaged cell; the ratio (R) between cpV (or citrine for D4ER) and ECFP mean fluorescence signal was calculated for each ROI (R = F530/F480).

Ca^{2+} imaging data are presented as:

- changes in emission ratio at 530/480 nm (R) normalized to the ratio at full Ca^{2+} saturation, calculated as:

$$R\% = (R - R_{min})/(R_{max} - R_{min}) \times 100$$

where R_{max} and R_{min} are the R values in permeabilized cells (or in the presence of the ionophore ionomycin) at saturating $[Ca^{2+}]$ and in the absence of Ca^{2+};

- $\Delta R/R_0$, for SOCE experiments; ΔR is the change of the cpV/ECFP emission intensity ratio at any time, R_0 is the fluorescence emission ratio at the time 0;
- $[Ca^{2+}]$, calculated as described in [34]: for D4ER, K_d = 321 μM and n (Hill coefficient) = 1.01 [28]; for Go-D1cpv K_d = 25 μM and n = 0.88 [32]; or medialGo-D1cpv K_d = 27 μM and n = 0.77 [31].

Data were analysed using Microsoft Excel and Origin 7.5 SR5 (OriginLab Corporation) to calculate rates and peaks.

2.4. Preparation of protein extracts and western blot analysis

Human fibroblasts or SH-SY5Y cells overexpressing PSs were solubilised in RIPA buffer (50 mM Tris, 150 mM NaCl, 1% Triton X-100, 0.5% deoxycholic acid, 0.1% SDS, protease inhibitor cocktail, pH 7.5) and incubated on ice for 30 min. Insolubilized material was spun down at 4000 g for 5 min at 4 °C. 40 μg of protein were loaded onto polyacrylamide gels and immunoblotted. Proteins were resolved by TruPAGE Precast Gels 4–12% (Sigma Aldrich) in TruPAGE TEA-Tricine SDS Running Buffer (Sigma Aldrich) and blotted onto a nitrocellulose membrane and probed with anti-STIM1 antibody (BD Transduction Laboratories Purified Mouse 1:250), anti-STIM-2 antibody (Sigma S8572 Rabbit 1:1000) or anti-actin antibody (Sigma A2228 Mouse 1:3000). The proteins are visualized in chemiluminescence using a secondary antibody anti-Mouse (Bio-Rad, 1:5000) or anti-Rabbit (Bio-Rad, 1:3000). Densitometry was performed using ImageJ software (National Institutes of Health). When indicated, 1 μM DAPT (N-[N-(3,5-Difluorophenacetyl)-L-alanyl]-S-phenylglycine t-butyl ester) has been added to the cultured medium overnight before protein extraction.

2.5. Immunocytochemistry

SH-SY5Y cells expressing PS2 and D4ER or Go-D1cpv or medialGo-D1cpv were fixed in Phosphate Buffered Saline (PBS) containing 4% paraformaldehyde for 15 min, incubated with 50 mM NH_4Cl for 20 min, permeabilized with 0.1% Triton X-100 in PBS for 3 min and then

blocked with 2% BSA and 0.2% gelatine for 30 min; PS2 was stained using an anti-PS2 antibody (Santa Cruz Biotechnology, Dallas, Texas, USA; 1:100). Alexa Fluor 555 conjugated goat anti-goat (Thermo Fisher Scientific) was applied for 1 h at room temperature. Coverslips were mounted using Mowiol (Sigma-Aldrich, Saint Louis, MI, USA). Images were collected at Leica TCS-SP5-II confocal system, equipped with a Plan Apo 100×/1.4 numerical aperture objective. For all images, pinhole was set to 1 Airy unit. The Argon laser line (488 nm) was used to excite the fluorescent proteins of the Cameleon sensors and the He/Ne 543 nm laser was used to excite the Alexa Fluor555 antibody. Confocal microscopy imaging was performed at 1024 × 1024 pixels, with a 200 Hz acquisition rate.

2.6. Materials

Thapsigargin, Bradykinin, Digitonin, EGTA and $CaCl_2$ were purchased from Sigma-Aldrich. CPA, ATP, DAPT and Ionomycin were purchased from Abcam. All other materials were analytical or of the highest available grade.

2.7. Statistical analysis

All data are representative of at least 3 experiments. Numerical values presented throughout the text are mean ± SEM (N = number of independent experiments or cells; ∗ = p < 0.05, ∗∗ = p < 0.01, ∗∗∗ = p < 0.001, unpaired Student's t test).

3. Results

3.1. The FAD-linked PS2-T122R mutant, but not PS1-A246E, reduces ER and medial-GA $[Ca^{2+}]$ resting levels in SH-SY5Y cells

PS2, both endogenous or transiently expressed, has been reported to localize in intracellular membranous compartments, mostly ER and GA [35,36]. In order to analyse, in SH-SY5Y cells, the intracellular localization of exogenously expressed PS2, both wt and carrying the pathological mutation T122R, the cDNA of PS2 (wt or T122R) was transiently co-transfected with those of Cameleons specifically targeted to the ER [28], the medial- [31] or the trans-GA [32]. PS2 (immunolabeled by a specific anti-PS2 antibody) co-localizes in part with each of the three fluorescent Ca^{2+} probes (Fig. 1), confirming that the protein, either wt or mutated, is localized in all the three compartments.

Single-cell analysis of Ca^{2+} handling was performed in cells co-expressing PS2 and one of the three probes, D4ER, medialGo-D1cpv or Go-D1cpv. Cells were excited at 425 nm and the emissions of the donor, ECFP, at 480 nm, and of the acceptor, cpV (or citrine for D4ER), at 540 nm were simultaneously recorded. The ratio between the fluorescent intensity emitted at 540 and 480 nm (R) is a function of the $[Ca^{2+}]$ experienced by the probe and provides a rapid qualitative estimate of the changes of this parameter over time (see Materials and Methods). To calibrate the R signal in terms of absolute $[Ca^{2+}]$ (see [34] for details), R values at very low (R_{min}) and very high (R_{max}) $[Ca^{2+}]$ need to be measured. To this end, cells were permeabilized with digitonin (or treated with the Ca^{2+} ionophore ionomycin) while perfused with a Ca^{2+}-free medium containing 0.5 mM EGTA, to reach R_{min} and finally, with a medium containing no EGTA and 3 mM $CaCl_2$ to reach R_{max}.

Representative traces of $[Ca^{2+}]$ changes in the three compartments are presented (Fig. 2A,C,E) as R changes, normalized to R_{max} and R_{min} (R%, see Materials and Methods). In panel 2 A (ER), cells were first challenged (in a Ca^{2+}-free medium and in the presence of EGTA) with the SERCA inhibitor CPA and the agonist bradykinin (BK), that caused a very rapid and large decrease of the signal to a level that was not further decreased by plasma membrane (PM) permeabilization with digitonin. Qualitatively, the response to BK plus CPA was identical in controls and cells expressing PSs, but the R starting values were clearly
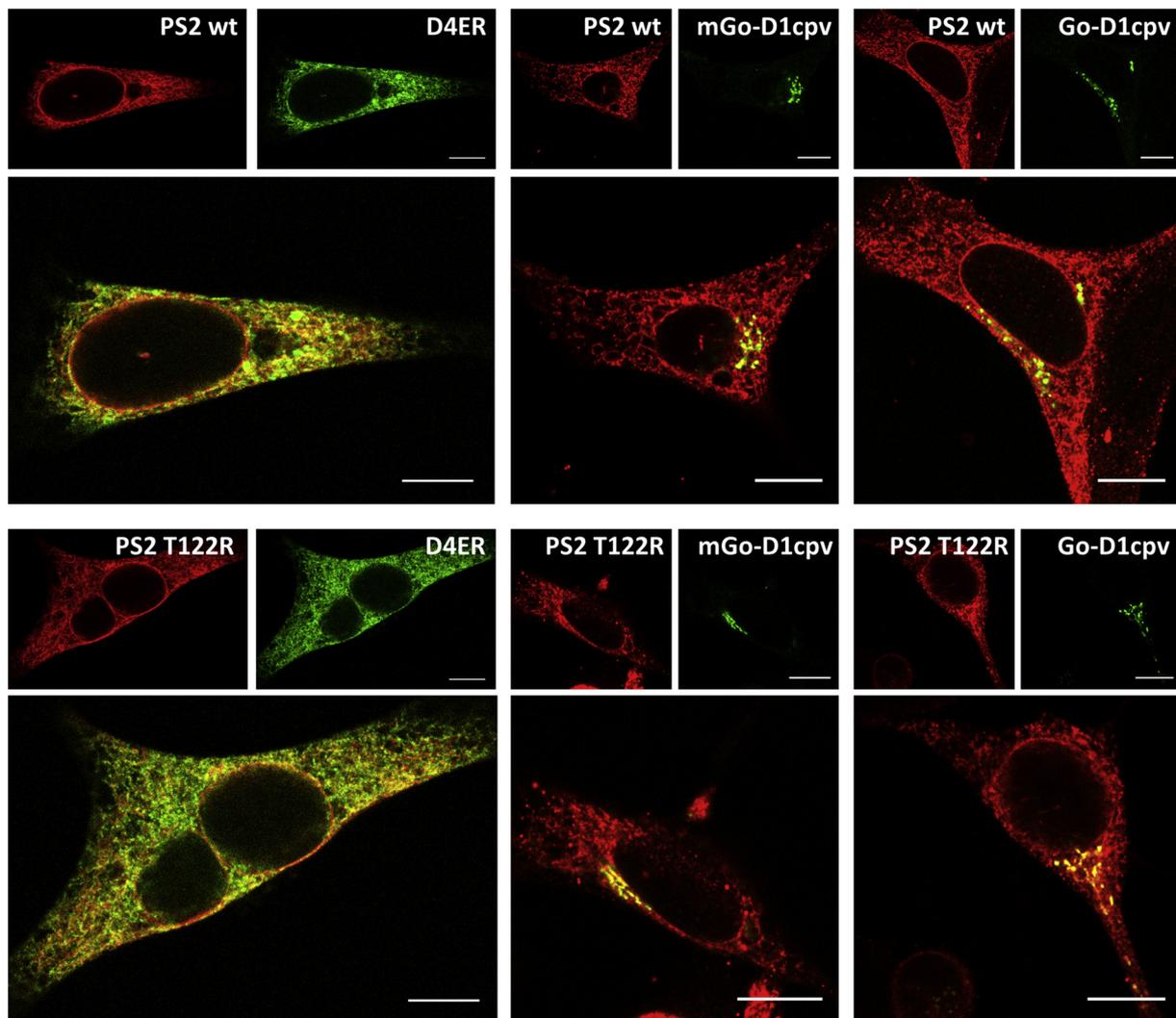
Fig. 1. Cameleon Ca^{2+} probes and PS2 co-localization in SH-SY5Y cells. Immunofluorescence of SH-SY5Y cells expressing PS2 (wt or T122R, as indicated) and one of the Cameleon probes (ER, medial-GA- or trans-GA-targeted, as indicated). PS2, either wt or T122R, was immunolabeled by an anti-PS2 antibody. Scale bar, 10 μm.

lower in cells expressing PS2 (wt or FAD-mutant). Panels 2C and 2E show the results obtained with cells expressing medial- or trans-GA-localized probe, respectively. In this case, the complete depletion of Ca^{2+} from the two GA compartments was obtained with ionomycin, given that CPA plus BK caused only a partial emptying of these GA regions (see Fig. 3C and [31,32]). The values of R$_{min}$ and R$_{max}$ obtained using ionomycin were not significantly different when digitonin was used instead (data not shown). As for the ER, also in the medial-GA, but not in the trans-GA, the initial R values in cells expressing PS2 (wt or FAD-mutant) were clearly lower, compared to those found in control and PS1-expressing cells. In the corresponding histograms (Fig. 2B,D,F), the values of resting [Ca^{2+}] are presented, calculated from R% values, using the previously reported K$_d$s [28,31,32], as described in Materials and Methods. Please note that, in these and the following experiments, despite the absolute values of R measured in the ER are similar or smaller than those in medial- and trans-GA, [Ca^{2+}] values after conversion are, as expected, higher in the ER. This is due to the higher K$_d$ of the probe used to monitor the [Ca^{2+}] within the ER, compared to those of the probes targeted to GA sub-compartments [28,31,32].

As already reported in BHK cells [28], also in SH-SY5Y cells the expression of either wt or the FAD-linked PS2-T122R mutant strongly reduced the ER Ca^{2+} level (Fig. 2A,B and Table S1). In particular, in terms of [Ca^{2+}], we observed a reduction, compared to control cells, of

40 and 46% in the case of PS2 wt and PS2-T122R expression, respectively. Cells expressing PS1, wt or carrying the FAD-linked mutation A246E, were also analysed and no effect on ER [Ca^{2+}] was observed (Fig. 2A,B and Table S1). Similar results were found in the medial-GA: expression of PS2, wt or T122R, led to markedly reduced R% values in resting conditions, that in terms of [Ca^{2+}] reflect a 72 and 70% reduction, respectively (Fig. 2C,D and Table S1). Again, no difference was found in the medial-GA Ca^{2+} content upon expression of PS1, either wt or mutated (Fig. 2C,D and Table S1). Trans-GA Ca^{2+} levels, instead, were not affected by the expression of any of the PSs expressed.

3.2. ER and medial-GA [Ca^{2+}] are affected in FAD-PS2 patient-derived fibroblasts

To investigate whether the reduction in ER and medial-GA [Ca^{2+}] observed in PS2-expressing SH-SY5Y cells could be due to protein overexpression, human fibroblasts from FAD patients carrying the mutations PS2-N141I or PS1-A246E (as well as fibroblasts from healthy age-matched controls) were similarly analysed (Fig. 3). In these cells, no variation in the total expression level of PSs has been reported [16].

In Fig. 3A, the same protocol used in Fig. 2A was applied. In Fig. 3C, before the complete depletion of the medial-GA by ionomycin addition, cells were treated with BK, which, as expected, caused only a partial
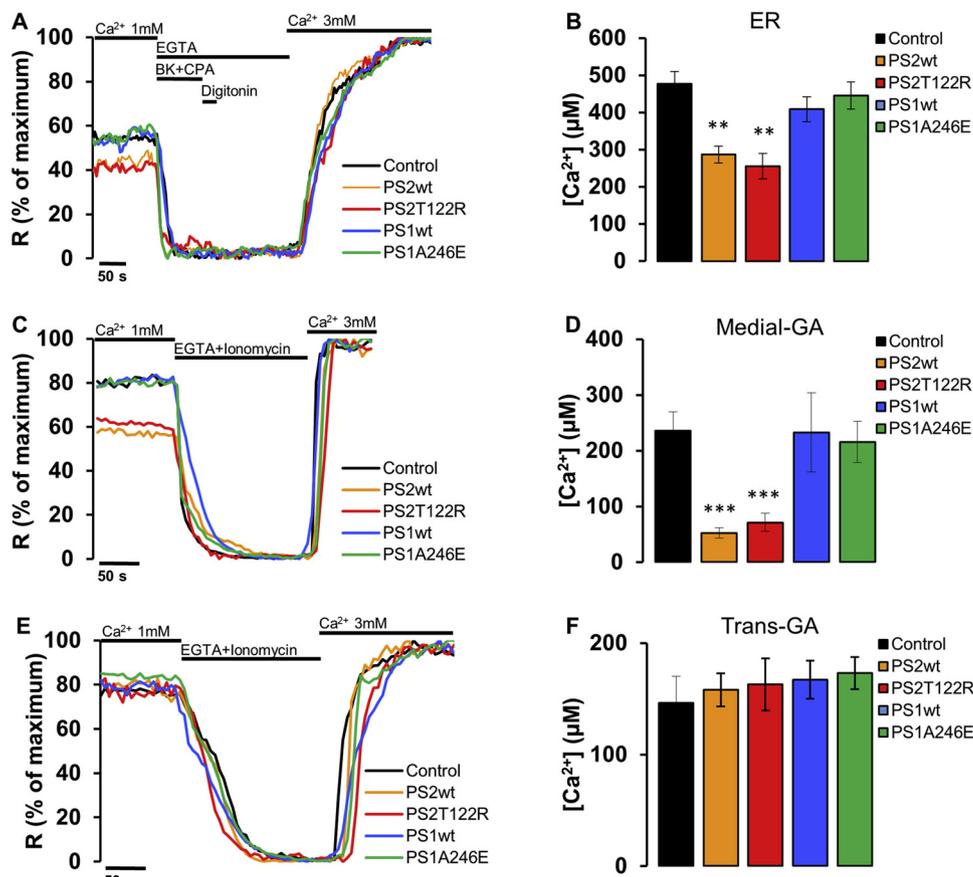
Fig. 2. Ca²⁺ dynamics in different intracellular compartments of SH-SY5Y cells. Ca²⁺ dynamics in SH-SY5Y cells, as detected by (**A, B**) ER-, (**C, D**) medial-GA- and (**E, F**) trans-GA-targeted Ca²⁺ probes. (**A, C, E**) Representative traces of a typical experiment performed in SH-SY5Y cells upon different additions (as indicated). Data are presented as R% (see Materials and Methods). (**B, D, F**) Histograms reporting the conversion in [Ca²⁺] of mean R% values in the different subcellular compartments: (**B**) ER, (**D**) medial-GA and (**F**) trans-GA. Data are presented as mean ± SEM of N ≥ 10 cells. ** p < 0.01; *** p < 0.0001.
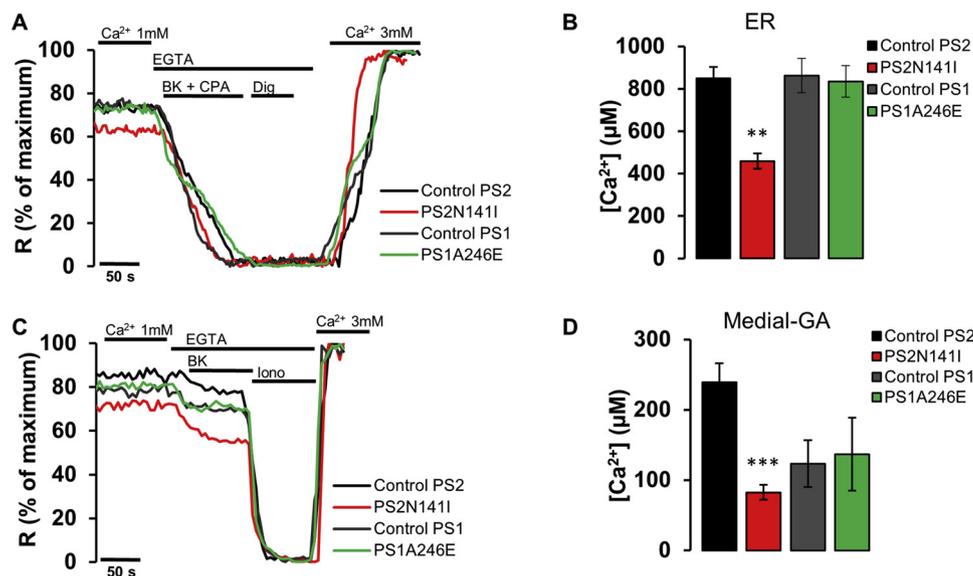

Fig. 3. Ca²⁺ dynamics in different intracellular compartments of FAD patient-derived fibroblasts. Ca²⁺ dynamics in human fibroblasts from FAD patients, or heathy controls, as detected by (**A, B**) ER- and (**C, D**) medial-GA-targeted Ca²⁺ probes. (**A, C**) Representative traces of a typical experiment performed in fibroblasts upon different additions (as indicated). Data are presented as R% (see Materials and Methods). (**B, D**) Histograms reporting the conversion in [Ca²⁺] of mean R% values in ER (**B**) and medial-GA (**D**) for PS2-N141I and age-matched control fibroblasts, and ER (**B**) and medial-GA (**D**) for PS1-A246E and age-matched control fibroblasts. Data are presented as mean ± SEM of N ≥ 14 cells. ** p < 0.01; *** p < 0.0001.

drop in the signal. When the R% values were calibrated in terms of [Ca²⁺], a reduction of 47% in resting [Ca²⁺]$_{ER}$ was measured in FAD-PS2-N141I patient-derived fibroblasts, compared to cells from an age-matched control (Fig. 3A,B and Table S2). On the contrary, no differences in resting [Ca²⁺]$_{ER}$ values were measured between controls and FAD-PS1-A246E human fibroblasts (Fig. 3A,B and Table S2). Similarly, FAD-PS2-N141I patient-derived fibroblasts showed a 71% reduced [Ca²⁺] in the medial-GA (Fig. 3C,D and Table S2), compared to control cells. There were instead no differences in medial-GA [Ca²⁺] between control and FAD-PS1-A246E fibroblasts (Fig. 3C,D and Table S2). Of note, the medial-GA [Ca²⁺] was significantly different between

fibroblasts from healthy individuals used as PS2 and PS1 age-matched controls. Despite we do not have a conclusive explanation for this difference, a high variability between human subjects is commonly reported and, in this specific case, it could be age-linked. Indeed, the PS2-age-matched control subject is 80 years old, significantly older than the PS1-matched control one (60 years old; see Materials and Methods).

3.3. FAD-PS2 mutants reduce ER and medial-GA Ca²⁺ uptake by inhibiting SERCA activity

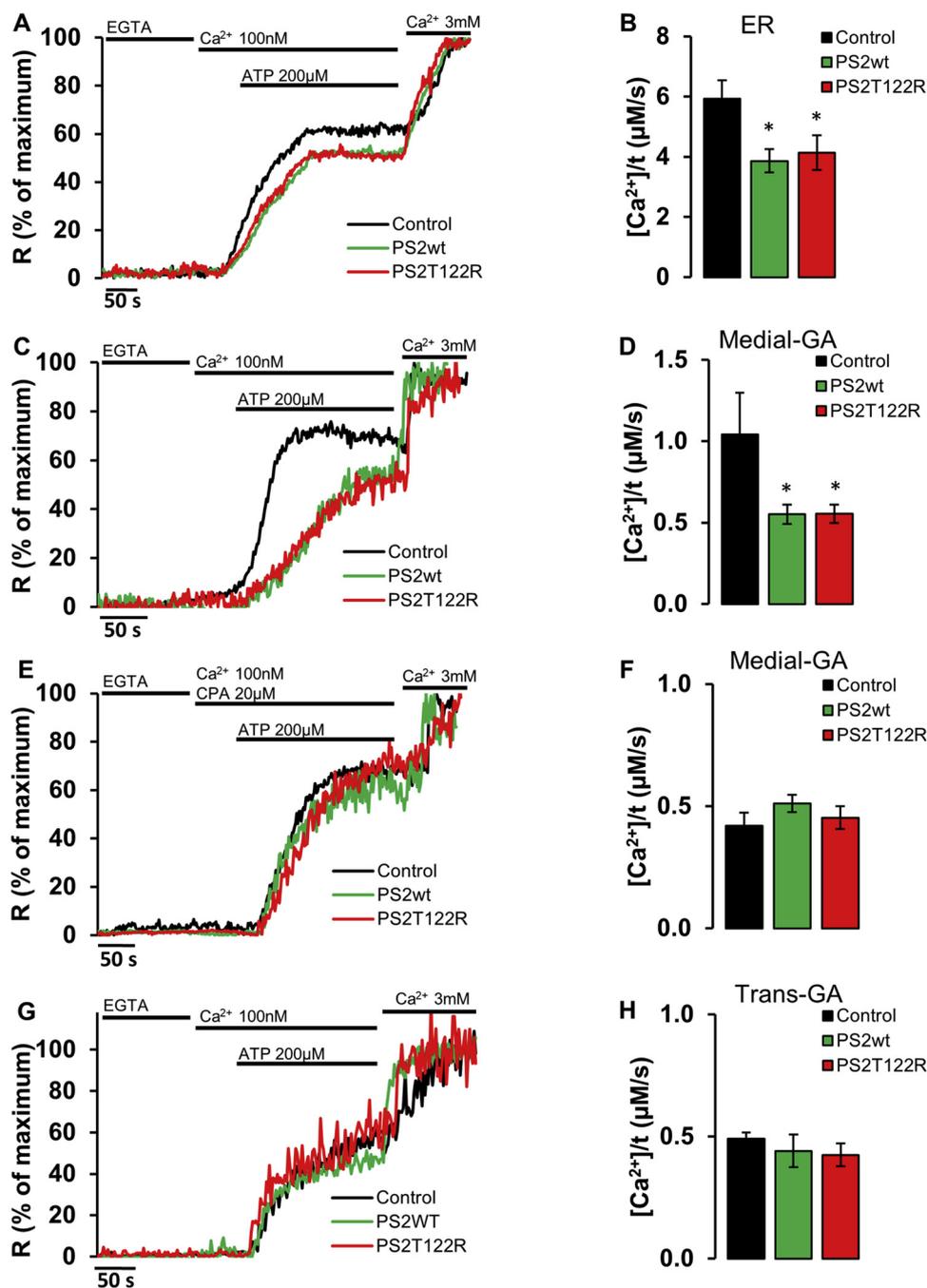To elucidate the molecular mechanisms underlying the reduction of

Fig. 4. Ca²⁺ refilling of different intracellular compartments in SH-SY5Y cells. Ca²⁺ refilling of intracellular stores in SH-SY5Y cells, as detected by (**A, B**) ER-, (**C, D, E, F**) medial-GA- and (**G, H**) trans-GA-targeted Ca²⁺ probes. (**A, C, E, D**) Representative traces of a typical experiment performed in SH-SY5Y cells upon different additions (as indicated): after intracellular Ca²⁺ store depletion, cells were permeabilized in an intracellular-like medium containing EGTA, then perfused with 100 nM Ca²⁺ in the presence of 200 μM ATP. Data are presented as R% (see Materials and Methods). (**B, D, F, H**) Histograms reporting the rate of Ca²⁺ refilling in the different conditions: (**B**) ER, (**D**) medial-GA (**F**) medial-GA in the presence of CPA and (**H**) trans-GA. Data are presented as mean ± SEM of N ≥ 5 cells. * p < 0.05.

ER and medial-GA Ca²⁺ content induced by PS2, we evaluated the efficacy of SERCA pump activity in these two compartments in SH-SY5Y cells co-expressing the D4ER, or the medialGo-D1cpv, probe and PS2 (wt or T122R; or the void vector as a control). Importantly, it has been previously demonstrated that the expression levels of the pump in control and FAD-PS2-expressing cells, as well as in brains of wt and FAD-PS2 transgenic mice, are indistinguishable [23,29]. Cells were pre-incubated in a Ca²⁺-free, EGTA-containing medium in the presence of the SERCA inhibitor CPA for 10 min, to induce intracellular Ca²⁺ stores depletion. Cells were then permeabilized, washed with an intracellular-like medium containing EGTA and perfused with Ca²⁺ (100 nM) in the presence of ATP (200 μM). Under these conditions, the [Ca²⁺], evaluated as R%, within the ER and medial-GA rapidly returned to a steady state of about 60–70% of the maximum level reached upon addition of 3 mM CaCl₂ (Fig. 4A,C). The expression of PS2, both wt and mutated, significantly reduced both the steady-state Ca²⁺ level reached within

the ER, as well as the rate of ER refilling (Fig. 4A,B and Tables S3). Similarly, in the medial-GA the two parameters were strongly reduced in PS2-, wt or mutated, expressing cells compared to controls (Fig. 4C,D and Tables S3). As expected, the expression of FAD-PS2-T122R (or PS2 wt) did not alter either the steady-state level reached upon a controlled refilling or the rate of luminal [Ca²⁺] increase within the trans-GA (Fig. 4G,H and Tables S3).

Altogether, these results suggest that the expression of wt or FAD-PS2-T122R decreases ER and medial-GA [Ca²⁺] likely by inhibiting the SERCA pump, confirming previous data [23,28,31,37]. On the contrary, trans-GA [Ca²⁺] is not affect by PS2 expression, suggesting that the trans-GA Ca²⁺ pump, the Secretory Pathway Ca²⁺ ATPase1 (SPCA1; [32,37,38]), is not inhibited. To confirm this conclusion, we transfected SH-SY5Y cells with the cDNA for the medial-GA Ca²⁺ probe together with PS2 (wt or FAD mutant), and applied the same protocol described above, except for the presence of the SERCA inhibitor CPA during the
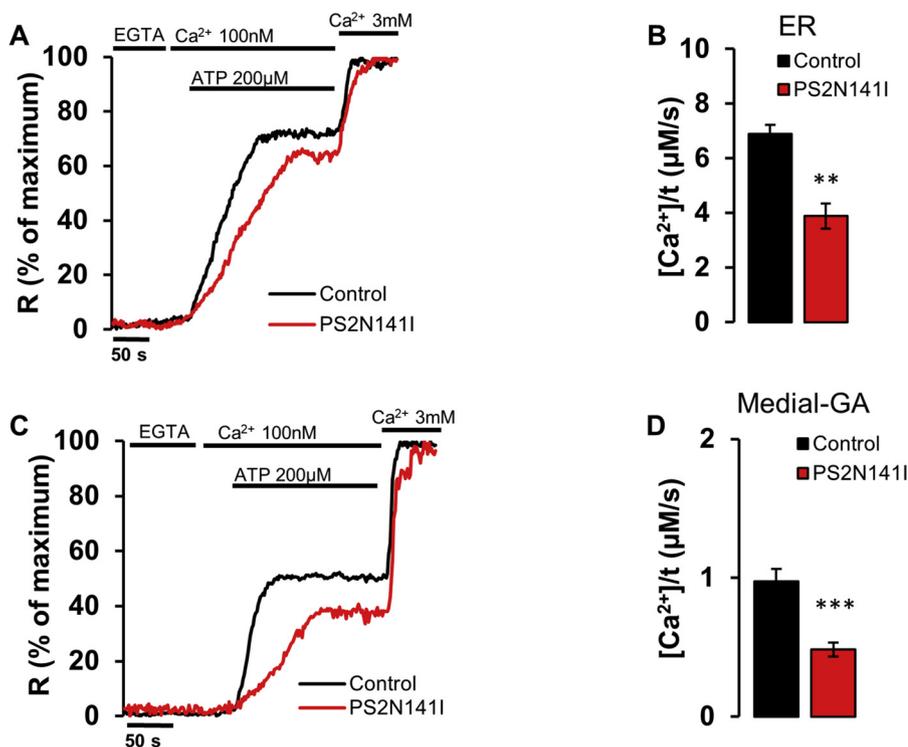
Fig. 5. Ca^{2+} refilling of different intracellular compartments in FAD patient-derived fibroblasts. Ca^{2+} refilling of intracellular stores in FAD-PS2-N141I patient-derived fibroblasts, and relative controls, as detected by (**A, B**) ER- or (**C, D**) medial-GA-targeted Ca^{2+} probes. (**A, C**) Representative traces of a typical experiment performed in fibroblasts upon different additions (as indicated): after intracellular Ca^{2+} stores depletion, cells were permeabilized in an intracellular-like medium containing EGTA, and then perfused with 100 nM Ca^{2+} in the presence of 200 μM ATP. Data are presented as R% (see Materials and Methods). (**B, D**) Histograms reporting the rate of Ca^{2+} refilling in (**B**) ER and (**D**) medial-GA. Data are presented as mean ± SEM of N ≥ 7 cells. ** p < 0.01; *** p < 0.0001.

Ca^{2+} uptake phase. In this condition, only SPCA1, the other pump responsible for medial-GA Ca^{2+} uptake [31], is able to pump Ca^{2+} inside the medial-GA lumen. As predicted, although in the absence of SERCA activity the rate of Ca^{2+} refilling and the steady state [Ca^{2+}] were reduced, neither of them was altered in PS2-expressing cells compared to controls, confirming that the activity of SPCA1 is not affected by PS2 expression (Fig. 4E,F and Tables S3).

Of note, comparing the refilling rate of medial-GA in the presence or in absence of CPA, similar values were obtained in PS2-expressing cells without the inhibitor (Fig. 4C,D) and in control or PS2-expressing cells treated with CPA (Fig. 4E,F), indicating that SERCA pump is almost completely inactivated by PS2 expression in this organelle.

Importantly, the SERCA pump activity was reduced also in FAD-PS2 patient-derived fibroblasts, compared to their controls: in fact, in both ER and medial-GA, the steady-state luminal [Ca^{2+}] upon Ca^{2+} refilling was lower than in controls and similarly, the Ca^{2+} refilling rate was reduced compared to controls (Fig. 5 and Tables S4). These results further demonstrate that FAD-linked PS2, expressed at physiological levels as in patient fibroblasts, is more efficient in SERCA inhibition than the wt protein.

3.4. Ca^{2+} leak from ER and medial-GA is not modified by FAD-PS2 mutants

Since the steady state of [Ca^{2+}] in intracellular stores depends on the balance between influx (*e.g.*, refilling mechanisms) and efflux (*e.g.*, leak) pathways, we investigated whether the reduced resting [Ca^{2+}] in ER and medial-GA observed in cell expressing FAD-PS2 were, at least in part, due to an altered passive Ca^{2+} leak. In order to flatten potential differences in Ca^{2+} leak due to different ER and medial-GA Ca^{2+} contents, as we found in control and PS2-expressing cells (Fig. 2A–D), control cells were incubated, before starting Ca^{2+} measurements, in an EGTA-containing medium for a time suited to partially deplete both the ER and the medial-GA (see Materials and Methods). After these treatments, the average starting Ca^{2+} content in the ER (264 ± 15 μM; n = 9) and medial-GA (45 ± 4 μM; n = 9) of pre-depleted control cells matched those of PS2 (wt or FAD-PS2) expressing cells (Fig. 6A, C).

Passive Ca^{2+} leak from the stores was then measured by incubating the cells in an extracellular-like medium containing EGTA and CPA, in order to inhibit SERCA-mediated Ca^{2+} uptake. The expression of PS2 (wt or mutated) did not affect the rate of passive Ca^{2+} leak pathways in neither the ER nor the medial-GA (Fig. 6 and Table S5). Noteworthy, in these and the previous experiments, the rates of luminal [Ca^{2+}] increase (and decrease) measured are underestimations of the total Ca^{2+} uptake rates (or releases). In fact, a large fraction of the Ca^{2+} taken up by the organelles is bound by luminal Ca^{2+} buffers, whose quantity and affinity is however still unknown. In particular, the initial rates of luminal [Ca^{2+}] increases (as measured after complete Ca^{2+} depletion of the organelles) are likely to be most underestimated, given that the luminal Ca^{2+} is very low and the buffering capacity maximal. These considerations allow explaining the paradoxical result that, in medial-GA, the rates of the initial Ca^{2+} refilling are lower than those of luminal Ca^{2+} leak at steady state.

3.5. FAD-PSs reduce SOCE activation and the expression level of STIM1

Since the filling of intracellular Ca^{2+} stores is also dependent on the specific Ca^{2+} entry from the PM activated by store depletion itself (*i.e.*, SOCE), we investigated the impact of FAD-linked PS mutants on this Ca^{2+} influx pathway. SH-SY5Y cells were transfected with wt or mutated PSs, or with an empty vector, as a control. Changes in cytosolic [Ca^{2+}] ([Ca^{2+}]$_c$) were monitored using the cytosolic FRET-based genetically encoded Cameleon probe D3cpv. To activate SOCE, ER Ca^{2+} depletion was induced by pre-incubating cells in an extracellular-like, Ca^{2+}-free, EGTA-containing, medium in the presence of the irreversible SERCA inhibitor thapsigargin (see Materials and Methods). Upon Ca^{2+} re-addition, SOCE was detected as a large [Ca^{2+}]$_c$ increase (Fig. 7A).

Fig. 7A shows representative Ca^{2+} traces, presented as ΔR/R$_0$ (see Materials and Methods). Average plateau values, reached after Ca^{2+} re-addition, revealed that the expression of both PS1 and PS2, either wt or mutated, similarly affect SOCE, causing a decrease of about 30%, compared to that measured in control cells (Fig. 7A and Table S6). The maximal rate of [Ca^{2+}]$_c$ increase was also calculated and was clearly decreased in PSs-expressing cells (Fig. 7C and Table S6).
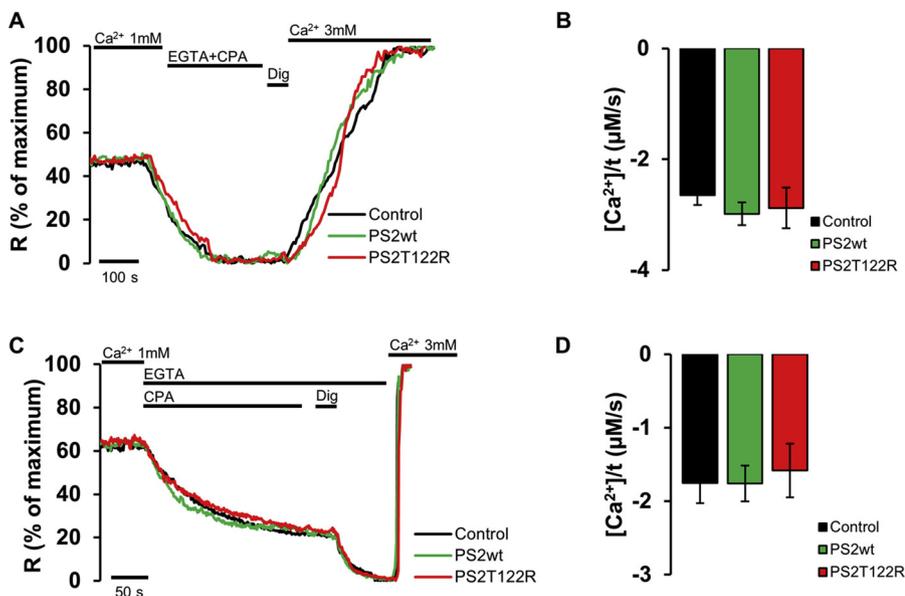
Fig. 6. Ca^{2+} leak of different intracellular compartments in SH-SY5Y cells. Ca^{2+} leak of intracellular stores in SH-SY5Y cells expressing PS2 (wt or T122R), and relative pre-depleted controls with similar Ca^{2+} content within ER (**A, B**) and medial-GA (**C, D**), as detected by specific Ca^{2+} probes targeted to the lumen of the specific organelle. (**A, C**) Representative traces of a typical experiment upon different additions (as indicated): passive Ca^{2+} leak was measured incubating cells in an extracellular-like medium containing EGTA (0.6 mM) and CPA (20 μM). Data are presented as R% (see Materials and Methods). (**B, D**) Histograms reporting rates of Ca^{2+} leak in the different conditions: (**B**) ER and (**D**) medial-GA. Data are presented as mean ± SEM of N ≥ 7 cells.

Alterations in PM potential can affect the rate and extent of SOCE, by altering the driving force for Ca^{2+} entry [39]. To exclude the possibility that PSs expression could affect PM potential, a set of experiments has been performed using a protocol similar to that described above, except that cells were perfused with a medium in which NaCl was iso-osmotically substituted by KCl (K$^+$-based medium; see Materials and Methods). Under these conditions, the PM potential collapses and differences in PM potential among cells are mostly abridged. Since, however, the driving force for Ca^{2+} entry is now decreased, the concentration of Ca^{2+} re-added upon store depletion was doubled with respect to the previous protocol (3 mM; Fig. 7D). Also in these conditions, the average Ca^{2+} plateau values measured after Ca^{2+} re-addition and the rate of Ca^{2+} entry were reduced upon PSs expression (Fig. 7E, F and Table S6).

FAD patients-derived fibroblasts carrying the PS1-A246E or the PS2-N141I mutation, and cells from aged-matched healthy controls, were similarly analyzed, activating SOCE using the same protocol described above. A clear reduction in both the Ca^{2+} plateau values and the rates of [Ca^{2+}]$_c$ increase was observed in both FAD PS1 and PS2 fibroblasts, compared to their age-matched controls (Fig. 8 and Table S7).

Similar experiments, but using a K$^+$-based medium, were also performed with these cells. However, the presence of L-type Voltage-Operated Ca^{2+} Channels (VOCCs; [40]), and the activation of a not

well-defined K$^+$-exchanger in fibroblasts (Greotti et al., unpublished results) prevented the possibility of applying this protocol to properly analyze SOCE.

With a lower steady-state [Ca^{2+}]$_{ER}$, PS2-expressing cells should show an activated SOCE at resting conditions and higher cytosolic Ca^{2+} levels, compared to control and PS1-expressing cells. We thus evaluated both parameters in control and PS1- or PS2-expressing SH-SY5Y cells. To this end, the following experimental protocol was applied: SH-SH5Y cells, control or expressing PS1 or PS2 (wt or FAD mutant) together with the cytosolic Cameleon probe D3cpv, were perfused in an extracellular Na$^+$-based saline and then in a K$^+$-based saline, both supplied with 1 mM CaCl$_2$. Ca^{2+} was then replaced by EGTA (0.6 mM) and, ultimately, CaCl$_2$ (3 mM) was re-perfused (Supplementary Fig. 1A). In the first part of the experiment, we evaluated R values at resting (Na$^+$ or K$^+$) conditions, while the last steps allowed the evaluation of SOCE at resting conditions, having excluded possible PM contributions. We found that the expression of PS1 or PS2 did not change resting Ca^{2+} levels both in physiological conditions (i.e. using an extracellular Na$^+$-based saline; Supplementary Fig. 1B), and in conditions that collapse PM potential (i.e. K$^+$-based medium; Supplementary Fig. 1C). Similarly, resting SOCE was unaffected by the expression of PSs (Supplementary Fig. 1D).

The ER Ca^{2+} sensor STIM1 and the pore-forming subunit of the PM
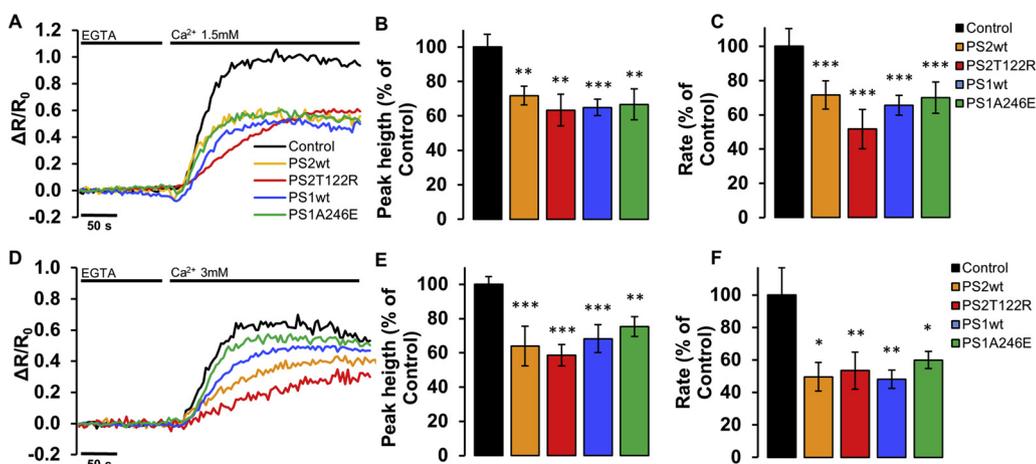

Fig. 7. Ca^{2+} dynamics induced by SOCE activation in SH-SY5Y cells expressing different PSs, and relative controls, as detected by the cytosolic Cameleon Ca^{2+} probe D3cpV. (**A, D**) Representative traces of a typical experiment performed in cells transfected with the cDNA for PSs, or the void vector: cells were pre-treated to empty intracellular stores, then perfused with a medium containing 1.5 mM (**A**) or 3 mM (**D**) CaCl$_2$. Data are presented as ΔR/R$_0$. (**B, C** and **E, F**) Histograms reporting (**B, E**) the average plateau values, measured as difference between plateau and basal levels, or (**C, F**) the rate of luminal [Ca^{2+}] increase normalized to controls, for each condition. (**D-F**) Cells were bathed in an extracellular K$^+$-based medium (see Materials and Methods). Data are presented as mean ± SEM of N ≥ 14 cells. * p < 0.05; ** p < 0.01; *** p < 0.0001.
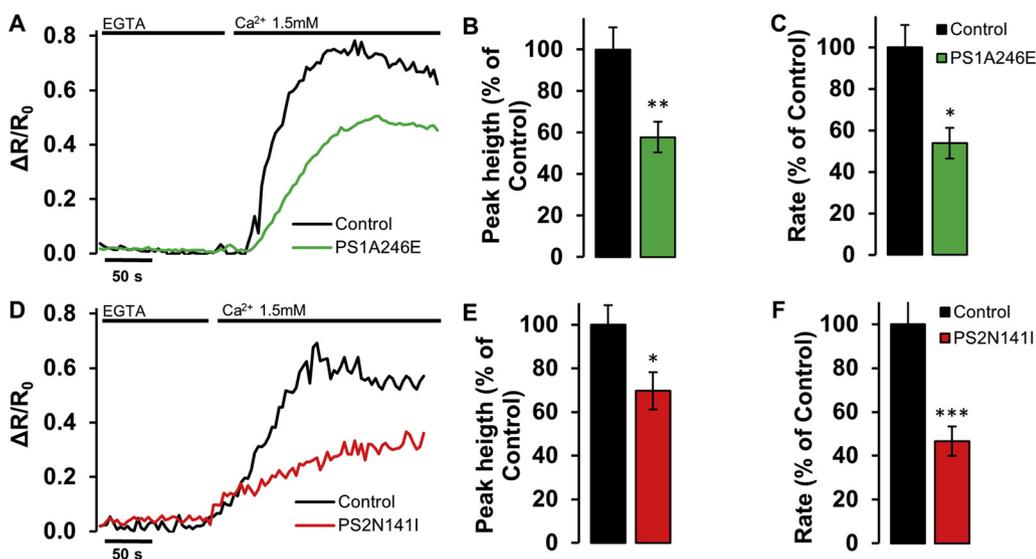
Fig. 8. Ca^{2+} dynamics induced by SOCE activation in FAD patient-derived fibroblasts, and relative controls, as detected by the cytosolic Cameleon Ca^{2+} probe D3cpV. (A–D) Representative traces of a typical experiment performed in fibroblasts from FAD patients carrying the PS1-A246E (A) or the PS2-N141I (D) mutation, compared to age-matched controls. Cells were pre-treated to empty intracellular stores and perfused with a medium containing 1.5 mM CaCl$_2$. Data are plotted as $\Delta R/R_0$. (B, C, E, F) Histograms show average peak values (B, E), measured as difference between peak and basal levels, or rates of [Ca^{2+}] increase (C, F), normalized to controls. Data are presented as mean ± SEM of N ≥ 14 cells. * p < 0.05; ** p < 0.01; *** p < 0.0001.
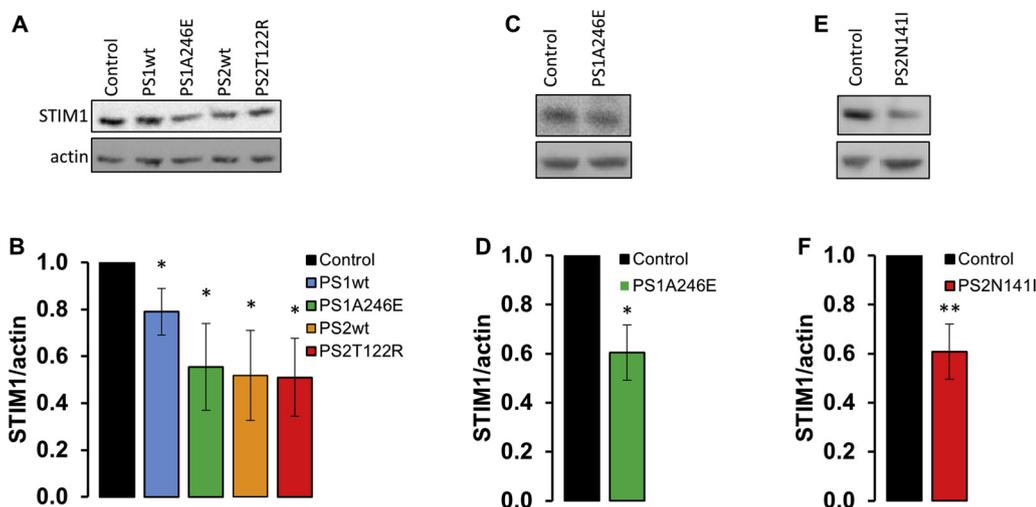

Fig. 9. STIM1 protein expression levels in different PS-expressing cells. STIM1 protein levels in PSs-expressing SH-SY5Y cells (A, B) and human FAD fibroblasts (C, F). Total proteins from wt and mutant PS-expressing cells, and relative controls, were extracted and analyzed by Western blotting. (A, C, E) Representative blots stained with antibodies anti-STIM1 and anti-actin, as a loading control. (B, D, F) Quantification of STIM1 protein levels, normalized to actin. Data are presented as mean ± SEM of N ≥ 4 independent experiments. * p < 0.05; ** p < 0.01.

channel Orai1 are the major molecular players in SOCE activation. To check whether alterations in the expression level of STIM1 could be involved in the decreased SOCE activation observed upon PSs expression, its protein levels were evaluated by Western blotting in SH-SY5Y cells overexpressing PSs. Compared to controls, a significant decrease in STIM1 protein level was observed in all the conditions tested (Fig. 9A,B). Similarly, a reduction of 40% in STIM1 protein level was calculated in FAD-PS1-A246E or FAD-PS2-N141I patient-derived fibroblasts, compared to their respective age-matched controls (Fig. 9C–F). A lower amount of STIM1 protein, compared to controls, was present also in PSs-expressing cells treated with the γ-secretase inhibitor DAPT (Supplementary Fig. 2), demonstrating that the observed reduction is not dependent on PSs γ-secretase activity. On the contrary, the expression levels of STIM2 protein, which has been proposed to have a role in setting ER [Ca^{2+}] [11], were not significantly different between FAD cell models and relative controls (Supplementary Fig. 3).

4. Discussion

The critical role of Ca^{2+} in AD pathogenesis originates from studies carried out more than 20 years ago, in which altered cytosolic Ca^{2+} responses in peripheral cells from patients with sporadic or familial forms of AD were reported [41,42]. Moreover, during the initial phases of aging, intracellular Ca^{2+} handling undergoes multiple changes [43],

which are dramatically amplified and anticipated in AD [42,44,45], converging in synaptic defects and memory impairments. Exaggerated Ca^{2+} rises were found in different cell and animal FAD models, leading to the formulation of the "Ca^{2+} overload" hypothesis for AD [46], that was also supported by additional data [21] (reviewed in [47]). This hypothesis, however, was later questioned by a number of groups reporting either no alteration or reduced [Ca^{2+}] in the ER of cells expressing wt or FAD-mutant PSs [13,16,17,23–27,29,48]. Foskett and coworkers suggested that the previously reported "Ca^{2+} overload" caused by FAD-PS expression was apparent and due to an exaggerated Ca^{2+} release caused by an increased sensitivity of inositol trisphosphate receptors (IP$_3$Rs) [48–51]. Finally, some attempts to clarify the PSs role in Ca^{2+} homeostasis have been carried out using KO models for both PS1 and PS2. No differences in ER Ca^{2+} levels and dynamics were found between wt and PSs double-KO (DKO) hippocampal neurons [52] or Mouse Embryonic Fibroblasts (MEFs) [27]. However, also in this case, contradictory results have been obtained on the amount of Ca^{2+} released from the ER in MEFs KO for PSs, which was found to be attenuated [53] or amplified [21].

Altogether these findings, while supporting a key role for Ca^{2+} dysregulation in AD pathogenesis, highlight the need to use specific organelle-targeted Ca^{2+} indicators to directly investigate intracellular stores Ca^{2+} dynamics. In addition, it is important to distinguish between the effects on Ca^{2+} handling due to protein overexpression, as in cell lines and most transgenic animals, from those dependent on the PS

mutations themselves, as in cells from heterozygous FAD patients. We thus carried out a detailed and quantitative single cell analysis of $[Ca^{2+}]$ in the ER and GA sub-compartments, using as models the neuronal cell line SH-SY5Y, transfected with wt or FAD-linked PSs, and fibroblasts from healthy donors or FAD patients. In addition, the effects of PSs on $[Ca^{2+}]_c$ caused by SOCE activation were investigated in the same cell models. The results obtained are unambiguous, in particular: i) overexpression of wt PS2, but not PS1, reduces the levels of ER and medial-GA luminal $[Ca^{2+}]$ by a negative control of the SERCA pump; ii) the effects of the expression of FAD-linked PS2 were qualitatively and quantitatively very similar to those obtained overexpressing the wt protein; iii) this phenotype was observed also in FAD-PS2 (but not in FAD-PS1) patient-derived fibroblasts that express the FAD- PS2 mutation in heterozygosis (thus presenting the same total PS2 protein level of controls [16]); iv) FAD-PS2 and FAD-PS1 mutants show no defect in Ca^{2+} handling of the trans-GA, a compartment where IP$_3$Rs and SERCA pumps are not expressed [32,37]. In conclusion, PS2, but not PS1, appears to be a negative regulator of the SERCA and the FAD-linked mutations confer to the protein a gain of function effect.

Regarding PSs-mediated modulation of SOCE, a number of FAD-linked PS1 mutants has been reported to decrease the specific Ca^{2+} influx rate in different cell models [12,13,15,18] and transgenic mice [14,54]. Similar conclusions have been reached for FAD-PS2 mutants [13,16,17,55], while SOCE is potentiated as a result of PSs KO or downregulation [18,54,56]. The effect of PSs on SOCE has been proposed to be both dependent and independent on γ-secretase activity [55,57]. We here confirm that both FAD PS1 and PS2 mutants decrease SOCE to similar extents, in both SH-SY5Y cells overexpressing the mutant protein and in FAD patient-derived fibroblasts. Data obtained in fibroblasts reveal that FAD-linked mutations (in either PS1 or PS2), compared to wt proteins, cause a "gain-of-function" phenotype resulting in a stronger SOCE inhibition.

The molecular target of PS1 and PS2 effect on SOCE has not been clarified yet. SOCE activation is, in fact, based on the interaction between ER-localized STIM proteins (STIM1 and STIM2), sensing Ca^{2+} levels within the ER, and PM Orai Ca^{2+} channels (Orai1, Orai2, Orai3; reviewed in [11]). Of note, STIM1 is the most effective isoform in triggering SOCE, whereas STIM2 is mainly devoted to maintaining ER resting $[Ca^{2+}]$. Previous work suggested that cellular levels of STIM proteins can be modulated by PSs [58–60]. In particular, an increased level of STIM1 has been found in MEFs KO for PSs [58] and attributed to variations in gene transcription or protein stability, somehow modulated by PSs [58]. Moreover, it has been proposed that SOCE is modulated by a γ-secretase-dependent mechanism because the pool of STIM1 recruited upon SOCE activation is a substrate of PS1-containing γ-secretase complexes [12]. Noteworthy, brains from sporadic AD (SAD) patients present decreased STIM1 levels, correlated with the progression of neurodegeneration [61]. We here found a significant decrease of STIM1 in both PSs-expressing SH-SY5Y cells and human FAD fibroblasts. However, the observed reduction in STIM1 levels was not dependent on γ-secretase activity since a lower amount of protein, compared to controls, was found also in FAD-PSs-expressing cells treated with the γ-secretase inhibitor DAPT.

Decreased $[Ca^{2+}]_{ER}$, induced by PS2 expression, and alterations in STIM1 protein expression levels, induced by both PS1 and PS2 expression, could affect cytosolic Ca^{2+} level and SOCE at resting conditions. We directly addressed this issue but we did not find any difference in these parameters between PSs-expressing cells and controls. The indistinguishable resting cytosolic Ca^{2+} level between controls and PSs-expressing cells implies that there is not a constitutive activation of this Ca^{2+} entry pathway. Moreover, the direct measurements of SOCE at resting condition, i.e., without depleting intracellular Ca^{2+} stores, further confirm that chronic ER Ca^{2+} depletion and/or the alteration in STIM1 protein level, does not affect resting SOCE. These results could be explained, independently of STIM1 expression levels, as an adaptive consequence of the prolonged reduction in steady-state $[Ca^{2+}]_{ER}$.

Interestingly, it has been previously demonstrated that long-term reductions of $[Ca^{2+}]_{ER}$, obtained by prolonged cell incubations with a low extracellular Ca^{2+}-containing medium, induce a decrease in SOCE [62]. Thus, in our FAD-PS2 cells, the reduction in SOCE appears critical to maintain a resting cytosolic $[Ca^{2+}]$ indistinguishable from that of control cells, despite a major reduction of $[Ca^{2+}]$ within the ER.

The lower intracellular store Ca^{2+} content and the reduced SOCE here described in cells expressing FAD-linked PSs mutants and in fibroblasts derived from FAD patients could have multiple consequences, critical for AD pathogenesis. Depleted intracellular Ca^{2+} stores, mainly ER and GA, could have detrimental effects on neuronal fate. Indeed, a correct $[Ca^{2+}]$ in ER and GA is fundamental for protein folding and synthesis [37,63]. Furthermore, Ca^{2+} is constitutively transferred from ER to mitochondria at specific sites in which the two organelles are closely apposed, i.e., mitochondrial associated membranes (MAMs, [7]). The correct ER to mitochondria Ca^{2+} shuttling enhances the Krebs cycle, sustaining ATP production and avoiding autophagy [64,65]. Due to their effect on ER Ca^{2+} content, FAD-PS2 mutants dampen mitochondrial Ca^{2+} rises upon cell stimulation [24]. This results in an impairment in total and mitochondrial ATP production, leading to an overall unbalanced energetic status of the cells ([66,67] and Rossi et al., unpublished results). The inability of mitochondria to produce the sufficient amount of energy to supply neurons demand could impair their functionality, potentially leading to neuronal death, thus contributing to neurodegeneration. On the other hand, due to the reported FAD-PS2 ability to potentiate ER-mitochondria tethering [24,25,29], a toxic mitochondrial Ca^{2+} overload could instead occur under some conditions. Finally, mitochondrial transport along microtubules is also mediated by Ca^{2+}-modulated adaptor proteins [68]; thus, mitochondria distribution within the cell, a process particularly important in neurons where organelles have to be recruited to active zones (i.e., synapses), is critically dependent on Ca^{2+} signalling. Indeed, alterations in mitochondrial functions (such as shape, bioenergetics and movements) have been reported to characterize several neurodegenerative disorders, including AD [66–69].

As far as SOCE is concerned, despite its debated physiological role in excitable cells, a growing body of evidence indicates that it is vital, regulating many neuronal functions [70], such as neuronal transcription factor activation in resting neurons [71], neurotransmitter release and synaptic plasticity in active cells [72], or dendritic spines maturation [73]. Moreover, two studies [74,75] have reported a role of STIM1 in the regulation of Cav1.2, a VOCC expressed in neurons, heart and skeletal muscle. Thus, alterations in this Ca^{2+} pathway, as those caused by FAD-PSs, might have critical effects on neuronal functionality in AD. Importantly, SOCE attenuation has been shown to reduce mushroom spines in hippocampal neurons from FAD-PS1 M146 V knock-in mice [59] and increase neurotoxic Aβ generation in cells bearing FAD-PS1 mutations [18]. On the other hand, the overexpression of SOCE molecular components in HEK-APP expressing cells has been shown to constitutively activate the Ca^{2+} influx and reduce [76] or increase [77,78] Aβ secretion, indicating a mechanistic relationship between SOCE and Aβ production, yet in the absence of FAD-PSs expression. Moreover, SOCE impairment has been reported also in astrocytes [79,80], human microglia [80] and in lymphoblasts from FAD patients [58], underlining a possible connection between PSs-related SOCE alterations and immunity dysregulations associated to AD [81]. Finally, the reduced level of STIM1 found in different AD cell models could also contribute to a defective Ca^{2+} homeostasis and an impairment in memory and learning, yet independently form SOCE activation. In fact, it has been reported that STIM1 expression levels regulate metabotropic glutamate receptors (mGluRs) 1/5-mediated refilling of ER Ca^{2+} stores [82,83] and contribute in regulating synaptic plasticity in mice [84]. STIM1 reduction is also associated to mitochondrial dysfunction and up-regulation of L-type VOCCs, causing an increased Ca^{2+} entry in response to depolarization [61].

A key question arising from the present data concerns the common

link between the effect of different PSs mutations on Ca^{2+} handling and the FAD phenotype. PS1 and PS2 mutants have similar stimulatory effects on IP$_3$Rs activation [48–51] and similar inhibitory effects on SOCE [12–18,54,55] (and the present paper). Concerning the other main intracellular Ca^{2+} releasing channel, the Ryanodine Receptor (RyR), both PSs modulate its expression and activity [10,29,85,86], although the latter has been reported to be differentially modulated by PS1 and PS2 [87] and causally downstream of the PSs effect on IP$_3$Rs [50]. Similarly, the two homologue proteins exert distinct effects on SERCA-dependent Ca^{2+} accumulation in the ER and medial-GA (PS2 inhibits and PS1 is without effect) and on ER-mitochondria tethering [24,25]. Thus, the two proteins appear to have distinct actions on different Ca^{2+} signalling pathways (as it has been found for other cell processes [10,88], including the activity of γ-secretase itself [89]), yet all converging in an overall dysregulated Ca^{2+} homeostasis and a common disease phenotype (although associated with different ages of onset [8]). Moreover, increasing evidence indicates that Ca^{2+} dysregulation is a common AD phenotype, reported also in SAD [10,42,45,90] representing the most frequent cases of the pathology. In this regard, our finding showing that the effects of FAD-PS2 mutants on multiple cellular Ca^{2+} pathways can be mimicked by high expression levels of wt PS2 [16,17,23,24] (and the present paper) might have significant implications for the pathogenesis of all the forms of AD. Indeed, SAD patient-derived cells show decreased expression levels of REST (Repressor Element 1-Silencing Transcription factor; [91]), a repressor of transcription modulating different genes, including the PS2 gene, *PSEN2*. REST has been proposed to be neuroprotective, repressing genes involved in cell death and AD pathology. Accordingly, high levels of REST correlate with increased longevity and preserved cognitive functions [92]. In SAD, as well as in aged samples, a loss of nuclear REST has been detected and associated with changes in the expression of pathogenic genes, *e.g.*, an increase in PS2 expression [93]. Hence, an up-regulation of PS2 transcript/protein in SAD patients and old individuals could mimic the phenotypes associated with FAD-PS2 mutants.

Author contributions

PP and TP conceived the work; EG, PC, AW performed experiments; DP, EG and PP analyzed data; EG, TP, PP and DP wrote the manuscript.

Conflict of interest

The authors declare that they have no conflicts of interest with the contents of this article.

Acknowledgments

Appendix A. Supplementary data

Supplementary material related to this article can be found, in the online version, at doi:https://doi.org/10.1016/j.ceca.2019.02.005.

References

[1] M. Goedert, M.G. Spillantini, A century of Alzheimer's disease, Science 314 (2006) 777–781.

[2] F. Panza, V. Solfrizzi, B.P. Imbimbo, G. Logroscino, Amyloid-directed monoclonal antibodies for the treatment of Alzheimer's disease: the point of no return? Expert Opin. Biol. Ther. 14 (2014) 1465–1476.

[3] J. Hardy, D.J. Selkoe, The amyloid hypothesis of Alzheimer's disease: progress and problems on the road to therapeutics, Science 297 (2002) 353–356.

[4] E.A. Schon, E. Area-Gomez, Mitochondria-associated ER membranes in Alzheimer disease, Mol. Cell. Neurosci. 55 (2013) 26–36.

[5] C. Giorgi, A. Danese, S. Missiroli, S. Patergnani, P. Pinton, Calcium dynamics as a machine for decoding signals, Trends Cell Biol. 28 (2018) 258–273.

[6] A. Secondo, G. Bagetta, D. Amantea, On the role of store-operated calcium entry in acute and chronic neurodegenerative diseases, Front. Mol. Neurosci. 11 (2018) 87.

[7] R. Filadi, P. Theurey, P. Pizzo, The endoplasmic reticulum-mitochondria coupling in health and disease: molecules, functions and significance, Cell Calcium 62 (2017) 1–15.

[8] R. Cacace, K. Sleegers, C. Van Broeckhoven, Molecular genetics of early-onset Alzheimer's disease revisited, Alzheimers Dement. 12 (2016) 733–748.

[9] M. Agostini, C. Fasolato, When, where and how? Focus on neuronal calcium dysfunctions in Alzheimer's Disease, Cell Calcium (2016).

[10] B.C. Tong, A.J. Wu, M. Li, K.H. Cheung, Calcium signaling in Alzheimer's disease & therapies, Biochim. Biophys. Acta Mol. Cell Res. (2018).

[11] J.W. Putney, Forms of store-operated calcium entry mediators, STIM and Orai, Adv. Biol. Regul. 68 (2018) 88–96.

[12] B.C. Tong, C.S. Lee, W.H. Cheng, K.O. Lai, J.K. Foskett, K.H. Cheung, Familial Alzheimer's disease-associated presenilin 1 mutants promote gamma-secretase cleavage of STIM1 to impair store-operated Ca2+ entry, Sci. Signal. 9 (2016) ra89.

[13] G. Zatti, A. Burgo, M. Giacomello, L. Barbiero, R. Ghidoni, G. Sinigaglia, C. Florean, S. Bagnoli, G. Binetti, S. Sorbi, P. Pizzo, C. Fasolato, Presenilin mutations linked to familial Alzheimer's disease reduce endoplasmic reticulum and Golgi apparatus calcium levels, Cell Calcium 39 (2006) 539–550.

[14] M.A. Leissring, Y. Akbari, C.M. Fanger, M.D. Cahalan, M.P. Mattson, F.M. LaFerla, Capacitative calcium entry deficits and elevated luminal calcium content in mutant presenilin-1 knockin mice, J. Cell Biol. 149 (2000) 793–798.

[15] I.F. Smith, J.P. Boyle, P.F. Vaughan, H.A. Pearson, R.F. Cowburn, C.S. Peers, Ca2+ stores and capacitative Ca2+ entry in human neuroblastoma (SH- SY5Y) cells expressing a familial Alzheimer's disease presenilin-1 mutation, Brain Res. 949 (2002) 105–111.

[16] M. Giacomello, L. Barbiero, G. Zatti, R. Squitti, G. Binetti, T. Pozzan, C. Fasolato, R. Ghidoni, P. Pizzo, Reduction of Ca2+ stores and capacitative Ca2+ entry is associated with the familial Alzheimer's disease presenilin-2 T122R mutation and anticipates the onset of dementia, Neurobiol. Dis. 18 (2005) 638–648.

[17] G. Zatti, R. Ghidoni, L. Barbiero, G. Binetti, T. Pozzan, C. Fasolato, P. Pizzo, The presenilin 2 M239I mutation associated with familial Alzheimer's disease reduces Ca2+ release from intracellular stores, Neurobiol. Dis. 15 (2004) 269–278.

[18] A.S. Yoo, I. Cheng, S. Chung, T.Z. Grenfell, H. Lee, E. Pack-Chung, M. Handler, J. Shen, W. Xia, G. Tesco, A.J. Saunders, K. Ding, M.P. Frosch, R.E. Tanzi, T.W. Kim, Presenilin-mediated modulation of capacitative calcium entry, Neuron 27 (2000) 561–572.

[19] E. Ito, K. Oka, R. Etcheberrigaray, T.J. Nelson, D.L. McPhie, B. Tofel-Grehl, G.E. Gibson, D.L. Alkon, Internal Ca2+ mobilization is altered in fibroblasts from patients with Alzheimer disease, Proc. Natl. Acad. Sci. U. S. A. 91 (1994) 534–538.

[20] R. Etcheberrigaray, N. Hirashima, L. Nee, J. Prince, S. Govoni, M. Racchi, R.E. Tanzi, D.L. Alkon, Calcium responses in fibroblasts from asymptomatic members of Alzheimer's disease families, Neurobiol. Dis. 5 (1998) 37–45.

[21] H. Tu, O. Nelson, A. Bezprozvanny, Z. Wang, S.F. Lee, Y.H. Hao, L. Serneels, B. De Strooper, G. Yu, I. Bezprozvanny, Presenilins form ER Ca2+ leak channels, a function disrupted by familial Alzheimer's disease-linked mutations, Cell 126 (2006) 981–993.

[22] O. Nelson, H. Tu, T. Lei, M. Bentahir, B. de Strooper, I. Bezprozvanny, Familial Alzheimer disease-linked mutations specifically disrupt Ca2+ leak function of presenilin 1, J. Clin. Invest. 117 (2007) 1230–1239.

[23] L. Brunello, E. Zampese, C. Florean, T. Pozzan, P. Pizzo, C. Fasolato, Presenilin-2 dampens intracellular Ca2+ stores by increasing Ca2+ leakage and reducing Ca2+ uptake, J. Cell. Mol. Med. 13 (2009) 3358–3369.

[24] E. Zampese, C. Fasolato, M.J. Kipanyula, M. Bortolozzi, T. Pozzan, P. Pizzo, Presenilin 2 modulates endoplasmic reticulum (ER)-mitochondria interactions and Ca2+ cross-talk, Proc. Natl. Acad. Sci. U. S. A. 108 (2011) 2777–2782.

[25] R. Filadi, E. Greotti, G. Turacchio, A. Luini, T. Pozzan, P. Pizzo, Presenilin 2 modulates endoplasmic reticulum-mitochondria coupling by tuning the antagonistic effect of mitofusin 2, Cell Rep. 15 (2016) 2226–2238.

[26] J.E. McCombs, E.A. Gibson, A.E. Palmer, Using a genetically targeted sensor to investigate the role of presenilin-1 in ER Ca2+ levels and dynamics, Mol. Biosyst. 6 (2010) 1640–1649.

[27] D. Shilling, D.O. Mak, D.E. Kang, J.K. Foskett, Lack of evidence for presenilins as endoplasmic reticulum Ca2+ leak channels, J. Biol. Chem. (2012).

[28] E. Greotti, A. Wong, T. Pozzan, D. Pendin, P. Pizzo, Characterization of the ER-Targeted low affinity Ca(2+) probe D4ER, Sensors (Basel) 16 (2016).

[29] M.J. Kipanyula, L. Contreras, E. Zampese, C. Lazzari, A.K.C. Wong, P. Pizzo, C. Fasolato, T. Pozzan, Ca2+ dysregulation in neurons from transgenic mice expressing mutant presenilin 2, Aging Cell 11 (2012) 885–893.

[30] C. Lazzari, M.J. Kipanyula, M. Agostini, T. Pozzan, C. Fasolato, Ab42 oligomers selectively disrupt neuronal calcium release, Neurobiol. Aging 36 (2015) 877–885.

[31] A.K. Wong, P. Capitanio, V. Lissandron, M. Bortolozzi, T. Pozzan, P. Pizzo, Heterogeneity of Ca2+ handling among and within Golgi compartments, J. Mol. Cell Biol. 5 (2013) 266–276.

[32] V. Lissandron, P. Podini, P. Pizzo, T. Pozzan, Unique characteristics of Ca2+ homeostasis of the trans-Golgi compartment, Proc. Natl. Acad. Sci. U. S. A. 107

(2010) 9198–9203.

[33] A.E. Palmer, M. Giacomello, T. Kortemme, S.A. Hires, V. Lev-Ram, D. Baker, R.Y. Tsien, Ca2+ indicators based on computationally redesigned calmodulin-peptide pairs, Chem. Biol. 13 (2006) 521–530.

[34] A.E. Palmer, R.Y. Tsien, Measuring calcium signaling using genetically targetable fluorescent indicators, Nat. Protoc. 1 (2006) 1057–1065.

[35] A. Doan, G. Thinakaran, D.R. Borchelt, H.H. Slunt, T. Ratovitsky, M. Podlisny, D.J. Selkoe, M. Seeger, S.E. Gandy, D.L. Price, S.S. Sisodia, Protein topology of presenilin 1, Neuron 17 (1996) 1023–1030.

[36] W. Zhang, S.W. Han, D.W. McKeel, A. Goate, J.Y. Wu, Interaction of presenilins with the filamin family of actin-binding proteins, J. Neurosci. 18 (1998) 914–922.

[37] P. Pizzo, V. Lissandron, P. Capitanio, T. Pozzan, Ca2+ signalling in the Golgi apparatus, Cell Calcium 50 (2011) 184–192.

[38] E. Zampese, P. Pizzo, Intracellular organelles in the saga of Ca2+ homeostasis: different molecules for different purposes? Cell. Mol. Life Sci. 69 (2012) 1077–1104.

[39] R. Penner, C. Fasolato, M. Hoth, Calcium influx and its control by calcium release, Curr. Opin. Neurobiol. 3 (1993) 368–374.

[40] L.B. Baumgarten, K. Toscas, M.L. Villereal, Dihydropyridine-sensitive L-type Ca2+ channels in human foreskin fibroblast cells. Characterization of activation with the growth factor Lys-bradykinin, J. Biol. Chem. 267 (1992) 10524–10530.

[41] C. Peterson, R.R. Ratan, M.L. Shelanski, J.E. Goldman, Altered response of fibroblasts from aged and Alzheimer donors to drugs that elevate cytosolic free calcium, Neurobiol. Aging 9 (1988) 261–266.

[42] Z.S. Khachaturian, Calcium hypothesis of Alzheimer's disease and brain aging, Ann. N.Y. Acad. Sci. 747 (1994) 1–11.

[43] E.C. Toescu, A. Verkhratsky, The importance of being subtle: small changes in calcium homeostasis control cognitive decline in normal aging, Aging Cell 6 (2007) 267–273.

[44] E.C. Toescu, M. Vreugdenhil, Calcium and normal brain ageing, Cell Calcium 47 (2010) 158–164.

[45] S. Camandola, M.P. Mattson, Aberrant subcellular neuronal calcium regulation in aging and Alzheimer's disease, Biochim. Biophys. Acta 1813 (2011) 965–973.

[46] F.M. LaFerla, Calcium dyshomeostasis and intracellular signalling in Alzheimer's disease, Nat. Rev. Neurosci. 3 (2002) 862–872.

[47] K. Honarnejad, J. Herms, Presenilins: role in calcium homeostasis, Int. J. Biochem. Cell Biol. 44 (2012) 1983–1986.

[48] K.H. Cheung, D. Shineman, M. Muller, C. Cardenas, L. Mei, J. Yang, T. Tomita, T. Iwatsubo, V.M. Lee, J.K. Foskett, Mechanism of Ca2+ disruption in Alzheimer's disease by presenilin regulation of InsP3 receptor channel gating, Neuron 58 (2008) 871–883.

[49] K.H. Cheung, L. Mei, D.O. Mak, I. Hayashi, T. Iwatsubo, D.E. Kang, J.K. Foskett, Gain-of-function enhancement of IP3 receptor modal gating by familial Alzheimer's disease-linked presenilin mutants in human cells and mouse neurons, Sci. Signal. 3 (2010) ra22.

[50] D. Shilling, M. Muller, H. Takano, D.O. Mak, T. Abel, D.A. Coulter, J.K. Foskett, Suppression of InsP3 receptor-mediated Ca2+ signaling alleviates mutant presenilin-linked familial Alzheimer's disease pathogenesis, J. Neurosci. 34 (2014) 6910–6923.

[51] D.O. Mak, K.H. Cheung, P. Toglia, J.K. Foskett, G. Ullah, Analyzing and quantifying the gain-of-function enhancement of IP3 receptor gating by familial alzheimer's disease-causing mutants in Presenilins, PLoS Comput. Biol. 11 (2015) e1004529.

[52] B. Wu, H. Yamaguchi, F.A. Lai, J. Shen, Presenilins regulate calcium homeostasis and presynaptic function via ryanodine receptors in hippocampal neurons, Proc. Natl. Acad. Sci. U. S. A. 110 (2013) 15091–15096.

[53] N.N. Kasri, S.L. Kocks, L. Verbert, S.S. Hebert, G. Callewaert, J.B. Parys, L. Missiaen, H. De Smedt, Up-regulation of inositol 1,4,5-trisphosphate receptor type 1 is responsible for a decreased endoplasmic-reticulum Ca2+ content in presenilin double knock-out cells, Cell Calcium 40 (2006) 41–51.

[54] J. Herms, I. Schneider, I. Dewachter, N. Caluwaerts, H. Kretzschmar, F. Van Leuven, Capacitive calcium entry is directly attenuated by mutant presenilin-1, independent of the expression of the amyloid precursor protein, J. Biol. Chem. 278 (2003) 2484–2489.

[55] Y. Akbari, B.D. Hitt, M.P. Murphy, N.N. Dagher, B.P. Tseng, K.N. Green, T.E. Golde, F.M. LaFerla, Presenilin regulates capacitative calcium entry dependently and independently of g-secretase activity, Biochem. Biophys. Res. Commun. 322 (2004) 1145–1152.

[56] L. Ris, I. Dewachter, D. Reverse, E. Godaux, F. Van Leuven, Capacitative calcium entry induces hippocampal long term potentiation in the absence of presenilin-1, J. Biol. Chem. 278 (2003) 44393–44399.

[57] C.R. Shideman, J.L. Reinardy, S.A. Thayer, Gamma-Secretase activity modulates store-operated Ca2+ entry into rat sensory neurons, Neurosci. Lett. 451 (2009) 124–128.

[58] L. Bojarski, P. Pomorski, A. Szybinska, M. Drab, A. Skibinska-Kijek, J. Gruszczynska-Biegala, J. Kuznicki, Presenilin-dependent expression of STIM proteins and dysregulation of capacitative Ca2+ entry in familial Alzheimer's disease, Biochim. Biophys. Acta 1793 (2009) 1050–1057.

[59] S.Y. Sun, H. Zhang, J. Liu, E. Popugaeva, N.J. Xu, S. Feske, C.L. White, I. Bezprozvanny, Reduced synaptic STIM2 expression and impaired store-operated calcium entry cause destabilization of mature spines in mutant presenilin mice, Neuron 82 (2014) 79–93.

[60] H. Zhang, S. Sun, L. Wu, E. Pchitskaya, O. Zakharova, K. Fon Tacer, I. Bezprozvanny, Store-operated calcium channel complex in postsynaptic spines: a new therapeutic target for alzheimer's disease treatment, J. Neurosci. 36 (2016) 11837–11850.

[61] C. Pascual-Caro, M. Berrocal, A.M. Lopez-Guerrero, A. Alvarez-Barrientos, E. Pozo-Guisado, C. Gutierrez-Merino, A.M. Mata, F.J. Martin-Romero, STIM1 deficiency is linked to Alzheimer's disease and triggers cell death in SH-SY5Y cells by upregulation of L-type voltage-operated Ca(2+) entry, J. Mol. Med. (Berl) 96 (2018) 1061–1079.

[62] P. Pinton, D. Ferrari, P. Magalhães, K. Schulze-Osthoff, F. Di Virgilio, T. Pozzan, R. Rizzuto, Reduced loading of intracellular Ca(2+) stores and downregulation of capacitative Ca(2+) influx in Bcl-2-overexpressing cells, J. Cell Biol. 148 (2000) 857–862.

[63] A. Carreras-Sureda, P. Pihan, C. Hetz, Calcium signaling at the endoplasmic reticulum: fine-tuning stress responses, Cell Calcium 70 (2018) 24–31.

[64] C. Cardenas, R.A. Miller, I. Smith, T. Bui, J. Molgo, M. Muller, H. Vais, K.H. Cheung, J. Yang, I. Parker, C.B. Thompson, M.J. Birnbaum, K.R. Hallows, J.K. Foskett, Essential regulation of cell bioenergetics by constitutive InsP3 receptor Ca2+ transfer to mitochondria, Cell 142 (2010) 270–283.

[65] A. Rossi, P. Pizzo, R. Filadi, Calcium, mitochondria and cell metabolism: a functional triangle in bioenergetics, BBA Mol. Cell Res. (2018).

[66] L.J. Martin, Mitochondrial and cell death mechanisms in neurodegenerative diseases, Pharmaceuticals 3 (2010) 839–915.

[67] M.J. Devine, J.T. Kittler, Mitochondria at the neuronal presynapse in health and disease, Nat. Rev. Neurosci. 19 (2018) 63–80.

[68] Z.H. Sheng, The interplay of axonal energy homeostasis and mitochondrial trafficking and anchoring, Trends Cell Biol. (2017).

[69] P. Theurey, P. Pizzo, The aging mitochondria, Genes (Basel) 9 (2018).

[70] J.W. Putney Jr., Capacitative calcium entry in the nervous system, Cell Calcium 34 (2003) 339–344.

[71] R. Hooper, B.S. Rothberg, J. Soboloff, Neuronal STIMulation at rest, Sci. Signal. 7 (2014) pe18.

[72] N.J. Emptage, C.A. Reid, A. Fine, Calcium stores in hippocampal synaptic boutons mediate short-term plasticity, store-operated Ca2+ entry, and spontaneous transmitter release, Neuron 29 (2001) 197–208.

[73] E. Korkotian, M. Oni-Biton, M. Segal, The role of the store-operated calcium entry channel Orai1 in cultured rat hippocampal synapse formation and plasticity, J. Physiol. 595 (2017) 125–140.

[74] C.Y. Park, A. Shcheglovitov, R. Dolmetsch, The CRAC channel activator STIM1 binds and inhibits L-type voltage-gated calcium channels, Science 330 (2010) 101–105.

[75] Y. Wang, X. Deng, S. Mancarella, E. Hendron, S. Eguchi, J. Soboloff, X.D. Tang, D.L. Gill, The calcium store sensor, STIM1, reciprocally controls Orai and CaV1.2 channels, Science 330 (2010) 105–109.

[76] W. Zeiger, K.S. Vetrivel, V. Buggia-Prevot, P.D. Nguyen, S.L. Wagner, M.L. Villereal, G. Thinakaran, Ca2+ influx through store-operated Ca2+ channels reduces alzheimer disease b-Amyloid peptide secretion, J. Biol. Chem. 288 (2013) 26955–26966.

[77] N. Pierrot, P. Ghisdal, A.S. Caumont, J.N. Octave, Intraneuronal amyloid-beta1-42 production triggered by sustained increase of cytosolic calcium concentration induces neuronal death, J. Neurochem. 88 (2004) 1140–1150.

[78] F. Al-Mousa, F. Michelangeli, Some commonly used brominated flame retardants cause Ca2+-ATPase inhibition, beta-amyloid peptide release and apoptosis in SH-SY5Y neuronal cells, PLoS One 7 (2012).

[79] C.I. Linde, S.G. Baryshnikov, A. Mazzocco-Spezzia, V.A. Golovina, Dysregulation of Ca2+ signaling in astrocytes from mice lacking amyloid precursor protein, Am. J. Physiol., Cell Physiol. 300 (2011) C1502–C1512.

[80] V. Ronco, A.A. Grolla, T.N. Glasnov, P.L. Canonico, A. Verkhratsky, A.A. Genazzani, D. Lim, Differential deregulation of astrocytic calcium signalling by amyloid-beta, TNFalpha, IL-1beta and LPS, Cell Calcium 55 (2014) 219–229.

[81] R.B. Maccioni, A. Gonzalez, V. Andrade, N. Cortes, J.P. Tapia, L. Guzman-Martinez, Alzheimer s disease in the perspective of neuroimmunology, Open Neurol. J. 12 (2018) 50–56.

[82] J. Hartmann, R.M. Karl, R.P. Alexander, H. Adelsberger, M.S. Brill, C. Ruhlmann, A. Ansel, K. Sakimura, Y. Baba, T. Kurosaki, T. Misgeld, A. Konnerth, STIM1 controls neuronal Ca(2+) signaling, mGluR1-dependent synaptic transmission, and cerebellar motor behavior, Neuron 82 (2014) 635–644.

[83] M.M. Lv, Y.C. Cheng, Z.B. Xiao, M.Y. Sun, P.C. Ren, X.D. Sun, Down-regulation of Homer1b/c attenuates group I metabotropic glutamate receptors dependent Ca(2) (+) signaling through regulating endoplasmic reticulum Ca(2)(+) release in PC12 cells, Biochem. Biophys. Res. Commun. 450 (2014) 1568–1574.

[84] G. Garcia-Alvarez, M.S. Shetty, B. Lu, K.A. Yap, M. Oh-Hora, S. Sajikumar, Z. Bichler, M. Fivaz, Impaired spatial memory and enhanced long-term potentiation in mice with forebrain-specific ablation of the Stim genes, Front. Behav. Neurosci. 9 (2015) 180.

[85] G.E. Stutzmann, I. Smith, A. Caccamo, S. Oddo, F.M. Laferla, I. Parker, Enhanced ryanodine receptor recruitment contributes to Ca2+ disruptions in young, adult, and aged Alzheimer's disease mice, J. Neurosci. 26 (2006) 5180–5189.

[86] D. Del Prete, F. Checler, M. Chami, Ryanodine receptors: physiological function and deregulation in Alzheimer disease, Mol. Neurodegener. 9 (2014) 21.

[87] A.J. Payne, S. Kaja, P. Koulen, Regulation of ryanodine receptor-mediated calcium signaling by presenilins, Receptors Clin. Invest. 2 (2015) e449.

[88] S.P. Duggan, J.V. McCarthy, Beyond gamma-secretase activity: the multifunctional nature of presenilins in cell signalling pathways, Cell. Signal. 28 (2016) 1–11.

[89] R. Sannerud, C. Esselens, P. Ejsmont, R. Mattera, L. Rochin, A.K. Tharkeshwar, G. De Baets, V. De Wever, R. Habets, V. Baert, W. Vermeire, C. Michiels, A.J. Groot, R. Wouters, K. Dillen, K. Vints, P. Baatsen, S. Munck, R. Derua, E. Waelkens, G.S. Basi, M. Mercken, M. Vooijs, M. Bollen, J. Schymkowitz, F. Rousseau, J.S. Bonifacino, G. Van Niel, B. De Strooper, W. Annaert, Restricted location of PSEN2/gamma-Secretase determines substrate specificity and generates an intracellular abeta pool, Cell 166 (2016) 193–208.

[90] L. Bojarski, J. Herms, J. Kuznicki, Calcium dysregulation in Alzheimer's disease, Neurochem. Int. 52 (2008) 621–633.

[91] T. Lu, L. Aron, J. Zullo, Y. Pan, H. Kim, Y. Chen, T.H. Yang, H.M. Kim, D. Drake, X.S. Liu, D.A. Bennett, M.P. Colaiacovo, B.A. Yankner, REST and stress resistance in ageing and Alzheimer's disease, Nature 507 (2014) 448–454.

[92] P. Baldelli, J. Meldolesi, The transcription repressor REST in adult neurons: physiology, pathology, and diseases, eNeuro 2 (2015).

[93] S. Kaja, N. Sumien, V.V. Shah, I. Puthawala, A.N. Maynard, N. Khullar, A.J. Payne, M.J. Forster, P. Koulen, Loss of spatial memory, learning, and motor function during normal aging is accompanied by changes in brain presenilin 1 and 2 expression levels, Mol. Neurobiol. 52 (2015) 545–554.